Mon. Not. R. Astron. Soc. **000**, 000–000 (0000) Printed 1 February 2008 (MN LATEX style file v1.4)

Thermal material in relativistic jets

A. Celotti[1⋆], Z. Kuncic[2], M.J. Rees[3], J.F.C. Wardle[4]
[1] *S.I.S.S.A., via Beirut 2–4, 34014 Trieste, Italy*
[2] *Australian National University Astrophysical Theory Centre, ACT 0200, Australia*[†]
[3] *Institute of Astronomy, Madingley Road, Cambridge CB3 0HA*
[4] *Physics Department, Brandeis University, Waltham, MA 02254, USA*

1 February 2008

ABSTRACT
The properties of thermal material coexisting with non–thermal emitting plasma and strong magnetic field in the powerful jets of Active Galactic Nuclei (AGN) are examined. Theoretical and observational constraints on the physical properties of this 'cold' component are determined. While the presence of a thermal component occupying a fraction $\sim 10^{-8}$ of the jet volume is possible, it seems unlikely that such a component is capable of contributing significantly to the total jet energy budget, since the thermal reprocessing signatures that should appear in the spectra have not, as yet, been detected.

Key words: galaxies: active - galaxies : jets - radiative processes

1 INTRODUCTION

Powerful, highly–collimated jets with relativistic flow speeds transport prodigious amounts of energy from the compact nuclei of active galaxies. According to the standard paradigm (Blandford & Rees 1978, Blandford & Königl 1979), these relativistic jets reveal themselves chiefly through emission by a non–thermal distribution of relativistic particles that are probably confined and also accelerated *in situ* by strong magnetic fields. While little is known of any other particle component which might contribute significantly to the global energetics and internal structure of jets in AGN, it is possible that there may be present, at least in small amounts, relatively cool material with a quasi–thermal distribution. The question then arises: to what extent can such material contribute to the reservoir of kinetic energy that powers the relativistic jets?

The answer to this question, apart from offering much needed insight into the physical conditions in relativistic jets, may also have important implications for the connection between jets in AGN and those in young stars and Galactic compact objects. Although morphologically similar to AGN jets, the jets in young stars are largely 'thermal' (e.g. Herbig Haro objects are seen mainly in emission lines rather than continuum emission) and are moving with sub–relativistic flow speeds (see Wilson 1993 for a review). Jets in Galactic compact objects generally exhibit properties that are intermediate between those of jets in young stars and AGN, emitting both thermal and non–thermal radiation; they move with flow speeds that are much higher than in young stars, sometimes reaching the relativistic velocities (e.g. the binary system SS 433, Vermeulen 1993; see also Mirabel & Rodriguez 1996) that are characteristic of AGN.

In AGN jets, it is plausible that at least some quasi–thermal material is present simply because the acceleration of particles to relativistic energies is unlikely to be 100 per cent efficient. Indeed, the acceleration might not be continuous; non–thermal particles that have cooled down (or initially constitute the low-energy end of the particle distribution spectrum) can thermalize before they are re–accelerated (e.g. Ghisellini, Guilbert & Svensson 1988; de Kool, Begelman & Sikora 1989). Some material might also be trapped at the base of jets as they form, while some is expected to be entrained from the external medium as jets propagate, following dynamical instabilities at the boundary. If this cooler material accumulates to high enough densities, the thermalization and radiative timescales can be much shorter than the dynamical timescales. Such thermal gas should then be capable of producing spectral signatures.

The optical–UV spectral energy distributions of radio–loud quasars (and those of their radio–quiet counterparts), suggest that there is a significant amount of thermal material, in the form of broad and narrow line emitting gas, at least in the immediate environments of jets (Wills 1996). In cases where spectral signatures are seen, however, this reprocessing gas is inferred to reside close to, but outside the jets (see Wilson 1993 for a review and also Walker, Rom-

⋆ E-mail: celotti@sissa.it
† The ANUATC is operated jointly by the Mount Stromlo and Siding Springs Observatories and the School of Mathematical Sciences.

ney & Benson 1994). This is most spectacularly shown by the HST images of narrow line emitting gas (Capetti et al. 1996).

To date, there exists no radiative or dynamical evidence to suggest that there may be thermal material actually inside relativistic jets in AGN. The most extreme case is with BL Lacs. Despite sharing common spectral properties with radio–loud quasars (e.g. power–law continua, rapid variability, high degrees of linear polarization – see Bregman 1990), their essentially featureless spectra offer few clues to the possibility that thermal matter may be present in or near their jets. It still remains unclear whether this is due to the powerful jet emission swamping any underlying reprocessing features or whether these objects are indeed devoid of significant amounts of thermal emitting plasma or ionizing radiation. Recent observations of weak broad emission lines in several sources (Stickel, Fried & Kühr 1993; Vermeulen et al. 1995; Robinson & Corbett 1996; Nesci & Massaro 1996) have provided some evidence for thermal gas associated with BL Lacs. Also, the presence of relatively cold outflowing material has been inferred from the observations of absorption features in the extreme ultraviolet (EUV) (Königl et al. 1995) and soft X–ray bands (Canizares & Kruper 1984, Krolik et al. 1985, Madejski et al. 1991)[‡]. However, at most mildly relativistic velocities are derived, again suggesting that the absorbing gas is likely located outside the jet or at its boundaries.

It is possible that the thermal matter content of jets in radio–loud quasars and BL Lacs is regulated by the structure of the internal magnetic field. Together with the non–thermal emitting particles and the strong radiation field, the magnetic field is likely to be a dominant component in the jet environment. Indeed, it is expected that the internal structure of jets becomes complex and inhomogeneous on small scales owing to its presence. The particle, radiation and magnetic field components plausibly coexist in a multiphase medium, similar to what is believed to prevail in the central magnetosphere and in the more distant line–emitting regions of AGN. A spectacular example of this complex internal structure comes from the high resolution observations of the jet in M87 (Biretta et al. 1995). These images reveal the presence of both large, regular emission sites and weaker substructure resembling magnetic filaments.

The role of magnetic fields in confining cool 'clouds' at the very centres of AGN was first pointed out by Rees (1987) and subsequently considered by Celotti, Fabian & Rees (1992). More recently, the physical and radiative properties of clouds of cool, magnetically confined material in a typical AGN magnetosphere have been studied in detail by Kuncic, Blackman & Rees (1996) and Kuncic, Celotti & Rees (1997). While some physical effects are similar to the case studied here, the environment, the dynamics, and the observational constraints are obviously quite different in the jet case.

In fact, in most or all of the observed wavebands, from radio to γ–rays, the spectral energy distribution of AGN known to have relativistic collimated jets seems to be dominated by radiation produced in the jet itself. The most likely radiation mechanisms reproducing the characteristics of the observed non–thermal spectra are synchrotron emission and inverse Compton scattering by relativistic electrons[§]. The scattering can be off either the synchrotron photons or a radiation field external to the jet, such as the soft photons from an underlying accretion disk or line emission scattered by diffuse electrons (see e.g. Sikora, Begelman & Rees 1994).

In this paper, we determine limits on the amount and physical properties of quasi–thermal cold material in a relativistic jet environment. We consider both observational constraints, which so far only allow us to set upper limits, and theoretical ones, which are based on thermal, radiative and dynamical arguments. The expected radiative signatures of thermal matter and their detectability are also discussed. In Sections 2 and 3, we consider constraints deriving from energetic, dynamical and radiative considerations on a 'macroscopic' level, while in Section 4, we briefly discuss the limits imposed by the 'microscopic' effects of diffusion. Observational considerations and results based on polarization measures are examined in Section 5. All the limits are compared and discussed in Section 6, and conclusions are drawn in Section 7.

2 ENERGETIC CONSIDERATIONS

The strongest limit on the total amount of any thermal material contained within a relativistic jet is imposed by the total kinetic power. If the global energetics of jets is dominated by three main components, namely electromagnetic fields, non–thermal relativistic particles and thermal gas all comoving with a bulk speed $\sim c$, then the total jet power is given by

$$L_{\rm jet} \gtrsim L_{\rm em} + L_{\rm nt} + L_{\rm t} \simeq \pi\phi^2 R^2 \Gamma^2 c (U_{\rm B} + U_{\rm p}) \,, \qquad (1)$$

where $L_{\rm em}, L_{\rm nt}, L_{\rm t}$ are the powers in the above three components, respectively, ϕ is the opening angle of the jet, Γ its bulk Lorentz factor and R is a measure of distance along the jet axis. The inequality takes into account any power dissipated e.g. in the form of radiation.

The total power can be re-expressed in terms of the energy densities in the field and particles, $U_{\rm B}$ and $U_{\rm p}$, respectively. $U_{\rm p}$ then represents the contribution of both the non–thermal (relativistic) and thermal (non–relativistic) components, and critically depends on the composition of the plasma. We assume that most protons are cold and that the relativistic electrons have a power–law distribution with typical energy index $\gtrsim 2$ (in the following we will assume it to be ~ 2, corresponding to a photon energy spectral index $\alpha \sim 0.5$) and with a minimum Lorentz factor $\gamma_{\rm e,min} \lesssim 10^3$. Under these assumptions, the power is dominated by the bulk kinetic energy of the proton component, so $U_{\rm p} \sim m_{\rm p} c^2 (n_{\rm nt} + f_{\rm v} n_{\rm t})$. In the case of a plasma composed mainly of electron–positron pairs, $U_{\rm p} \sim 2 m_{\rm e} c^2 (n_{\rm nt} \langle\gamma_{\rm e}\rangle + f_{\rm v} n_{\rm t} m_{\rm p}/m_{\rm e})$ where $\langle\gamma_{\rm e}\rangle$ is the average electron Lorentz factor and $f_{\rm v}$ is

[‡] Recent observations with the SAX satellite also show signs of absorption in the soft X–ray band of the radio–loud quasar 3C 273, Grandi et al. 1997).

[§] Interestingly, it has been argued (Eilek & Caroff 1979) that these cooling processes in particular can stabilize relativistic plasma against thermal instability triggered by the presence of localized regions of cool gas.

the volume filling factor of the thermal material (the non–thermal plasma is assumed to fill the volume of the jet).

According to eq. (1), the total jet power implies a maximum *average* gas density

$$\langle n_{\rm max,jet}\rangle \sim (7\times10^9) L_{\rm jet,46}\phi_{-1}^{-2}R_{14}^{-2}\Gamma_{10}^{-2} \qquad {\rm cm}^{-3}\,, \qquad (2)$$

where we have assumed reference values of $L_{\rm jet} = 10^{46}L_{\rm jet,46}\,{\rm erg\,s^{-1}}$, $R = 10^{14}R_{14}$ cm, $\Gamma\sim\delta = 10\Gamma_{10}$ (where δ is the Doppler factor) and $\phi = 0.1\phi_{-1} \simeq \Gamma_{10}^{-1}$. This suggests the possibility that an energetically significant gas component could then be present in a relativistic jet in the form of very small and extremely dense clumps or 'clouds'. Typical total jet luminosities of the order of 10^{46} erg s^{-1} have been assumed on the basis both of the total power which can be extracted from a $10^8 M_\odot$ black hole and the estimate of the jet kinetic power on pc and extended scales (e.g. Rawlings & Saunders 1991; Celotti & Fabian 1993).

We also expect magnetic fields to play a significant role. A tangled or quasi–isotropic field component is likely to be responsible for the acceleration of particles to non–thermal energies. On the other hand, a large scale, ordered field, possibly anchored in an accretion disk, may be responsible for the collimation and acceleration of jets (see e.g. the review by Blandford 1993). The strength of a comoving magnetic field that carries a power $L_{\rm jet}$ as Poynting flux is typically

$$B \simeq (2\times10^4) L_{\rm jet,46}^{1/2}\phi_{-1}^{-1}R_{14}^{-1}\Gamma_{10}^{-1} \qquad {\rm G}. \qquad (3)$$

Any thermalized material that becomes trapped by such a strong field in a relativistic jet is bound to be subjected to dynamical forces and instabilities, which would produce clumped structures comoving with the jet. These structures would quickly come into pressure balance with the surroundings and would effectively be confined by the field stresses. The condition of pressure equilibrium then imposes a maximum density, which for gas with an internal plasma parameter $\beta \gg 1$, is

$$n_{\rm max,press} \sim (3\times10^{17}) B_4^{*2}T_5^{-1}R_{14}^{-2} \qquad {\rm cm}^{-3}, \qquad (4)$$

where a reference value $T \simeq 10^5 T_5$ K has been assumed for the temperature of the gas (see Section 3.1) and $B_4 = 10^{-4}B$ G. Here and in the following we indicate quantities estimated at R_{14} with an asterisk. Note that the constraint above applies to the effective density of the material, independent of its degree of 'clumpiness'. A comparison with the limit imposed by the total jet power shows that the condition of pressure balance gives a more stringent limit on the density in cold material, $n_{\rm t}$ for filling factors $f_{\rm v} \lesssim 10^{-8}$. This would then corresponds to $n_{\rm max,jet} \sim (7\times10^{17}) L_{\rm jet,46}\phi_{-1}^{-2}R_{14}^{-2}\Gamma_{10}^{-2}f_{\rm v,-8}^{-1}$ cm^{-3} where $f_{\rm v,-8} = 10^8 f_{\rm v}$.

In the following sections, we indeed argue that cold thermal gas is most likely to occupy only a fraction $f_{\rm v} \ll 1$ of the jet volume. In other words, the magnetic fields in relativistic jets are capable of providing an effective confining mechanism for an energetically significant amount of gas at the very high densities that are compatible with small volume filling factors. Furthermore, we show (in Section 3.1) that these densities are sufficiently high to sustain cool temperatures whilst such 'clouds' are immersed in the intense non–thermal radiation field of the jet.

3 MACROSCOPIC PROPERTIES

Hereafter, we assume the presence of dense clouds in an AGN jet environment at a distance R from the central massive object under the condition of particle and field conservation (i.e. $n_{\rm nt} \propto R^{-2}$ and $B \propto R^{-1}$). Although the limits discussed so far are independent of the specific spatial distribution or individual geometry of the clouds, we assume for simplicity that they are spherical with a radius r. Realistically, however, the clouds are likely to be filamentary or tube like, elongated along the field direction, so that r represents a measure of the pressure scaleheight or the characteristic dimension transverse to the magnetic field. We consider constraints on the possible physical conditions (namely the density and dimension) for the cold clouds to exist and survive during their propagation along a jet.

3.1 Temperature and density

Despite the intense radiation field which prevails in a relativistic jet environment, any thermal material can rapidly equilibrate at the equivalent blackbody temperature of the radiation field provided the gas density is sufficiently high that two–body radiative processes become more efficient than particle–photon interactions. For clouds comoving with the jet, the photon field could be dominated either by the local non–thermal radiation emitted by the ambient relativistic plasma or by the quasi–thermal radiation external to the jet.

An estimate of the cloud electron temperature can therefore be obtained by considering the energy density of radiation as measured in the cloud frame. This would be of the order of $U_{\rm rad} \sim (3\times10^4) L_{\rm obs,46}\delta_{10}^{-3}\phi_{-1}^{-1}R_{14}^{-2}$ erg cm^{-3} (if R is estimated by variability timescales then $U_{\rm rad} \propto \delta^{-5}$), where $L_{\rm obs,46}$ is a reference value for the observed (beamed) radiative luminosity. On the other hand, an external field of, say, $L_{\rm ext,45} = 10^{-45}L_{\rm ext}$ erg s^{-1} in a region of 10^{15} cm, would lead to $U_{\rm rad,ext} \sim (3\times10^5) L_{\rm ext,45}R_{15}^{-2}\Gamma_{10}^2$ erg cm^{-3}. The equivalent blackbody temperature would then be expected to be in the range $T_{\rm bb} \sim (10^4 - 10^5)$ K. Clearly, the equilibrium temperature could be a function of R, depending on the local radiation field. An attempt to calculate a plausible radiative equilibrium temperature at various distances by using the code CLOUDY, has lead to electron temperatures in the range estimated above. In the following a reference value $T_5 = 10^{-5}T$ K will be used, at all R.

This temperature can therefore be attained by clouds with densities such that the bremsstrahlung cooling timescale is shorter than the Compton heating timescale. The minimum density required for clouds to cool is thus

$$n_{\rm min,cool} \simeq (2\times10^{14}) U_{\rm rad}T_5^{-1/2} \qquad {\rm cm}^{-3}\,, \qquad (5)$$

where it has been assumed that the local non–thermal field is energetically dominated by γ–ray photons with energies $\sim m_{\rm e}c^2$. As blazar spectra are typically dominated either by the synchrotron/blue bump component in the optical–UV band or the Compton component at typically GeV energies, the internal radiation field could in fact have a significantly different Compton temperature and consequently the above estimate of $n_{\rm min,cool}$ is uncertain. Furthermore the scattering radiation can be mainly due to an external photon field (as in the case of high Γ).

Note that in the range of densities considered here, the radiative timescales are smaller than the typical dynamical timescales, so that spectral signatures could arise.

3.2 Scaleheights

For pressure equilibrium to be maintained and restored after any perturbation, clouds have to be sufficiently small that their sound–crossing response time is shorter than the characteristic dynamical timescale. This implies a maximum cloud size

$$r_{\rm max,sound} \simeq 10^9 R_{14} T_5^{1/2} \Gamma_{10}^{-1} \qquad {\rm cm}\,. \tag{6}$$

However, any amount of material trapped in the jet environment close to the central source would be subjected to strong radiative, magnetic and inertial forces, the balance of which would determine a typical scaleheight in the resultant direction. A cloud of entrained material would feel the dynamic pressure from the bulk flow of the jet which would be $\sim \Gamma^2 (c/v_{\rm s})^2 (n_{\rm nt}/n_{\rm t}) g$, where g is the gravitational acceleration and $v_{\rm s}$ the sound speed, and would expand (in the comoving frame) as this ram pressure decreases, until the bulk speed is achieved.

Forces due to radiation can also be dynamically important at the centres of AGN. The intense radiation field in the innermost regions can prevent the jet flow from rapidly accelerating to values of Γ exceeding about 10, due to the Compton drag felt by the non–thermal particles as they scatter off aberrated photons, emitted from the inner regions of an accretion disk or the more distant broad line region (Phinney 1987; see also Sikora et al. 1996b). Indeed, most observational properties of AGN jets (e.g. one–sidedness, superluminal proper motions and γ–ray emission) can be accounted for with $\Gamma \sim 3-10$. Radiation drag might also be expected to affect any cooler, denser material immersed in the intense radiation field. Such material, however, would be more susceptible to radiative (bremsstrahlung) absorption than to Compton scattering. If the low–frequency photons that are absorbed are mainly those emitted by the ambient non–thermal plasma in the jet, the analogous drag effect on the absorbing thermal material would be negligible (since the synchrotron photons are highly anisotropic and therefore suffer little relativistic aberration). Instead, the material would feel a net radiative acceleration $a \sim g \int {\rm d}\nu (\sigma_{{\rm abs},\nu}/\sigma_{\rm T})(L_\nu/L_{\rm Edd})$ until it reaches its terminal velocity, where $\sigma_{\rm abs}$ and $\sigma_{\rm T}$ are the absorption and scattering cross sections, respectively, and $L_{\rm Edd}$ is the reference Eddington luminosity. This acceleration depends on the radiation field but could reach $10^{4-6} g$ (Kuncic et al. 1996; see also Ghisellini et al. 1990 for the analogous effect of synchrotron absorption).

The detailed description of the dynamics of a cloud is quite complex and beyond the scope of this paper. What is relevant here is that the resultant acceleration a can easily be several orders of magnitude higher than g, leading to an estimate of the typical scaleheight

$$h \sim \frac{g}{a} h_{\rm grav} \simeq (6\times 10^6) \frac{g}{a} M_8^{-1} T_5 R_{14}^2 \qquad {\rm cm}\,, \tag{7}$$

where $M = 10^8 M_\odot M_8$ is the mass of the central black hole. This implies that in the inner part of jets, thermal plasma can have inhomogeneities on scales no larger than centimeters.

3.3 Spatial configuration

As already mentioned, the spatial distribution of any thermal material in a relativistic jet strongly depends on the structure of the magnetic field. If the thermal gas is diamagnetic ($\beta \gg 1$), it would not necessarily follow the kinematics of the magnetic and relativistic particle components. Such material, however, would be slowly penetrated by the field; in this condition the dynamical coupling would be effective and the compression of material would be limited by the internal field amplification.

Magnetic forces associated with poloidal fields could squeeze the plasma into filaments with a small covering factor, which could then be accelerated outwards along the field lines (e.g. Emmering et al. 1992). At large distances, however, the transverse toroidal component of the field dominates and this is favorable to cloud confinement by the tangential stresses associated with the curvature of the field lines. We would then expect a much larger covering factor over the jet cross–sectional area.

Almost independently of the specific geometry, we can derive limits on the distribution of thermal gas. By combining the constraint on the total power derived in eq. (2), which imposes a maximum particle density, with the minimum density required by the condition that the plasma is able to effectively radiate extra heat due to conduction from the relativistic phase (see Section 4.1), we can estimate an upper limit on the volume filling factor:

$$f_{\rm v} \lesssim (7\times 10^{-6}) n_{\rm nt,9}^{*-1} \langle\gamma_{\rm e}\rangle^{-1} T_5^{1/2} L_{\rm jet,46} \phi_{-1}^{-2} \Gamma_{10}^{-2}\,. \tag{8}$$

Here, $\langle\gamma_{\rm e}\rangle m_e c^2$ is the average energy of the relativistic particles (the Coulomb interactions are dominated by non–thermal particles with lowest energies) and $n_{\rm nt}^* = 10^9 n_{\rm nt,9}^*$ is their number density (at R_{14}). Hereafter the non–thermal particle density is estimated as the maximum allowed by the limits imposed on the total jet power, assuming particle conservation (and a constant acceleration efficiency at all R), i.e. $n_{\rm nt}(R) = 10^9 n_{\rm nt,9}^* R_{14}^{-2}$.

Similar limits on $f_{\rm v}$ are also derived from the minimum density required for clouds to cool in the strong radiation field, as given by eq. (5). Thus, any cool (and necessarily dense) gas could readily fill a small fraction of the jet volume, the filling factor being roughly comparable with the typical values for the reprocessing material responsible for the broad line emission.

3.4 Dynamics

Cold material confined by a tangential field would tend to comove with the bulk flow of a jet. However, in a situation where the cold component is in relative motion, with speed $v_{\rm c}$ with respect to the relativistic bulk flow, as during an acceleration phase, Kelvin–Helmholtz instabilities can lead to an effective mixing of the cold and relativistic phases and the consequent rapid heating of the cold

gas ¶. The disruptive effect of the instability could be suppressed for densities at which its typical growing time is longer than the cloud sound crossing time, i.e. $n_{\rm min,K-H} \gtrsim (5\times10^{16}) n^*_{\rm nt,9} T_5^{-1} R_{14}^{-2} (v_{\rm c}/c)^2\,{\rm cm}^{-3}$.

Clouds could also be subjected to instability due to the curvature of the magnetic field lines (analogous to the Rayleigh–Taylor instability for ordinary fluids). However, this depends on the details of the local field structure. Finally, shocks could form once the material reaches the highly relativistic jet speed.

4 MICROPHYSICAL CONSTRAINTS

The survival of cool clouds in a relativistic jet can be also severely threatened at a microphysical level by diffusion, which acts across the large gradients in particle density, temperature and magnetic field at the boundary of the confined gas. Note that, due to the strong magnetic field, any thermal gas at densities $n_{\rm t} \lesssim 10^{18}{\rm cm}^{-3}$ can be effectively treated as a globally neutral plasma confined by the field for any r larger than $\sim$ cm.

In this section we consider the effect of transfer of energy into the clouds due to both the relativistic plasma surrounding the thermal gas and the high energy radiation. Furthermore, the diffusion of the magnetic field and the expansion of the gas along its direction impose lower limits respectively on the dimension and mass of material not 'evaporating' within a dynamical timescale.

4.1 Diffusion

Relativistic particles can readily penetrate a cool, thermal phase embedded within a jet and then effectively transfer energy, providing a source of heat, through Coulomb collisions. This diffusive process would ultimately heat an entire cloud of cool gas. However, on the radiative and dynamical timescales relevant here, the diffusion would be effective only over dimensions $d(t_{\rm brem}) \simeq (5\times10^7) T_5^{1/4} n^{*-1}_{\rm t,15} \langle\gamma_e\rangle R_{14}^2$ cm and $d(t_{\rm dyn}) \simeq 10^{10} R_{14}^{3/2} n^{*-1/2}_{\rm t,15} \langle\gamma_e\rangle \Gamma_{10}^{-1/2}$ cm, respectively. An appropriate Coulomb factor of $\ln\Lambda \sim 10$ and a thermal particle density compatible with the constraints presented above have been assumed‖. Clouds can then maintain their cold temperature if significantly larger than these diffusion lengths.

Alternatively, smaller clouds can survive and not 'evaporate' if dense enough to efficiently radiate the energy input provided by the relativistic particles. The minimum density required is thus

$$n_{\rm min,diff} \simeq 10^{15} n^*_{\rm nt,9} \langle\gamma_e\rangle^{-1/2} T_5^{-1/2} R_{14}^{-2} \quad {\rm cm}^{-3}\,. \tag{9}$$

In other words, material with sufficiently high densities is not dramatically affected by the presence of the ambient relativistic plasma. The latter, however, would lose some of its internal energy as low–energy particles thermalize and effectively condense into the cool clouds.

An even more relevant heating agent, which is not affected by the presence of a strong field, has been discussed by Kuncic et al. (1996) in the case of magnetospheric clouds. This is the Coulomb heating provided by electron–positron pairs formed in clouds as a consequence of $\gamma-\gamma$ interactions. However, the observed copious γ–ray emission from radio–loud AGN indicates that jets are optically thin to photon–photon pair production, in natural agreement with the evidence of relativistic motion of the emitting plasma. Furthermore, suggestions that the observed γ–ray emission is due to the superposition of spectra from compact regions in an inhomogeneous jet (e.g. Blandford & Levinson 1995), seem to be at odds with the lack of observed reprocessed radiation at lower energies. Heating of cool material by electron–positron pairs in AGN jets is therefore unlikely to be important.

Finally, as a consequence of a non zero resistivity, any cold plasma would tend to diffuse and smooth gradients over the scale size of the field. This scale has then to be typically larger than $r_{\rm min,diffB} \gtrsim 20\ T_9^{-3/4} \Gamma_{10}^{-1/2} R_{14}^{1/2}$ cm to avoid the field penetrating the clouds within a dynamical timescale.

On the other hand, the particles can propagate along the direction of field lines. This implies that material confined in a magnetic filamentary/tube–like structure would progressively disperse, typically at the sound speed. Ultimately the filament can become so thin that diffusion across the field is effective and it completely disperses on a timescale $\lesssim t_{\rm dyn}$. Therefore, in order for the cold phase to survive long enough to propagate in the jet, a minimum amount of material has to be initially clumped. This corresponds to a minimum mass (at R_{14}) only of the order of

$$M \gtrsim 10^6 R_{14}^2 T_5^{1/2} n^*_{\rm t,15} \Gamma_{10}^{-1} \quad {\rm g}\,. \tag{10}$$

Note that the limit on the mass flux imposed by the constraint on the total jet power corresponds to Γ_{10}^{-1} the mass accreted at roughly the Eddington limit, $\dot{M} \lesssim 10^{24} L_{\rm jet,46} \Gamma_{10}^{-1}$ g, i.e. $2\times10^{-2} M_\odot$ yr^{-1}.

5 OBSERVATIONAL CONSTRAINTS

Significant amounts of thermal gas should produce observable spectral signatures which can provide a diagnostic of jet composition. Depending on R, we expect different observational constraints to prevail. In this Section, we examine the possible radiative signatures of thermal material in AGN jets, in terms of emission, absorption and Faraday rotation.

5.1 Column density limit

X–ray and EUV spectral observations of radio–loud quasars and BL Lacs have so far failed to reveal convincing evidence of excess absorption, by material in the jet, with respect to that produced by the Galactic hydrogen column density. Spectral features in the BL Lac object PKS 2155–304 (and a few others BL Lacs) at EUV (Königl et al. 1995) and soft X–ray energies (around 0.5-0.6 keV; e.g. Canizares & Kruper 1984, Krolik et al. 1985, Madejski et al. 1991) are best interpreted as variable absorption by gas moving at most at mildly relativistic speeds, possibly in a wind rather than in the jet itself. Recently, some authors (e.g. Elvis et al.

¶ Whittle & Saslaw (1986) (and references therein) pointed out the stabilizing effect of magnetic fields with respect to Kelvin–Helmholtz instability.

‖ In the direction perpendicular to the magnetic field lines, the diffusion effect is negligible owing to suppression by a factor equal to the ratio of collisional to gyro frequencies.

1994, Cappi et al. 1997 and references therein) have claimed the presence of excess absorption in soft X–rays that may be intrinsic to high redshift radio–loud quasars, with an $N_{\rm H}$ in the range $\sim (1-50)\times 10^{21}$ cm^{-2}. However, this material too is inferred to be outflowing at subrelativistic speeds and it is possibly located at large scales (Elvis et al. 1996). The lack of absorption in the X–ray band strongly limits the presence of neutral material along the line of sight of most sources to typical $N_{\rm H}\sim n_{\rm t}\phi R f_{\rm v}\lesssim 10^{20-21}$ cm^{-2}.

Note that the energetics constraint given by eq. (2) leads to an upper limit on the column density of $N_{\rm H}\lesssim (7\times 10^{22})L_{\rm jet,46}\phi_{-1}^{-1}R_{14}^{-1}\Gamma_{10}^{-2}$ cm^{-2}, which is higher than that allowed from observations, unless the plasma is highly ionized or most of the X–ray radiation is produced at distances $R\gg R_{14}$. **

5.2 Free–free absorption

Dense, cold material along the line of sight in an AGN jet would absorb both thermal and non–thermal radiation up to a characteristic frequency (for $\nu\lesssim (2\times 10^{16})T_5\delta_{10}$ Hz)

$$\nu_{\rm brem}(R)\simeq (8\times 10^{13})T_5^{-3/4}\delta_{10}n^*_{\rm t,15}f_{\rm v,-8}^{1/2}\phi_{-1}^{1/2}R_{14}^{-3/2}\ {\rm Hz}\,, \quad (11)$$

which is adequate for a high covering factor, for which an absorption feature can be detected in the observed spectrum. Highly clumped material could therefore easily absorb radiation up to the optical band in the inner regions of the jet.

In particular the observable effects of bremsstrahlung absorption strongly depend both on the covering factor of the material and on the structure of the non–thermal emitting region. If the synchrotron spectrum is produced in a single region and the clouds covering factor is $\lesssim 1$, the non–thermal radiation would be absorbed below $\nu_{\rm brem}$ (as estimated with $f_{\rm v}\lesssim 1$) only in proportion to the covered area. For higher covering factors, on the other hand, the spectrum would tend flatten toward ν^{-2} below the absorption frequency. More realistically, however, the observed radiation may be due to the superposition of spectra produced at different positions along an inhomogeneous jet (e.g. Blandford & Königl 1979; see Königl 1989 for a review of the different models proposed). In this case, any observable effect would of course depend on whether or not the absorbing thermal gas is co–spatial with the location where most of the radiation at that frequency is emitted. The detailed predictions here depend on the assumed gradients in the jet emissivity. In the case where thermal clouds (with the same physical properties) occupy a large fraction of the jet volume, the expected effect is a steep cutoff below $\nu_{\rm brem}$, proportional to the spatial extension of the cold material in the jet.

High brightness temperatures typical of the non–thermal emission in blazars suggest that induced Compton scattering can also be a competing process in depleting the low frequency photons. However, this would dominate over free–free absorption only for clouds with sizes $r\lesssim (2\times 10^3)\nu_{12}^{-0.5}T_5^{3/2}T_{\rm b,12}n^*_{\rm nt,9}R_{14}^{-3}n^{*-2}_{\rm t,15}$ cm, where $T_{\rm b}=10^{12}T_{\rm b,12}$ K is the brightness temperature of the radiation field at a frequency $\nu=10^{12}\nu_{12}$ Hz.

** Here and in the following we consider optical depths in the direction perpendicular to the jet axis because of the relativistic aberration of the observed emission. In other words we assume the factor for the aberration correction $\delta\sin\theta\sim 1$.

5.3 Synchrotron self–absorption

Clearly bremsstrahlung absorption would affect the emitted spectrum at each R if $\nu_{\rm brem}\gtrsim\nu_{\rm syn}$, where $\nu_{\rm syn}$ is the synchrotron self–absorption frequency. If the non–thermal emission is produced in an inhomogeneous jet structure, with different regions contributing at different observed bands, the local non–thermal radiation will be self absorbed up to a characteristic frequency (e.g. Blandford & Königl 1979)

$$\nu_{\rm syn}(R)\simeq (2\times 10^{14})\phi_{-1}^{1/3}\delta_{10}^{1/3}(\gamma_{\rm e,min}n^*_{\rm nt}B^{*2})^{1/3}R_{14}^{-1}\quad {\rm Hz}\,, \quad (12)$$

where $n_{\rm nt}$ and B have been normalized to the typical values derived from VLBI observations.

5.4 Faraday Rotation

Another signature of the presence of thermal material is its effect on the polarization of the synchrotron radiation. Its plane of polarization would be rotated through an angle $\chi=(2\times 10^4)n_{\rm t}f_{\rm v}Bf_{\rm B}R\phi\delta^2\nu^{-2}$ rad, where $f_{\rm B}$ takes into account reversals in direction of the magnetic field.

The importance of this effect at different distances R can be estimated by determining the frequency at which the rotation angle of the polarization vector is, say $\chi\sim 1$ rad:

$$\nu_{\rm F}(R)\simeq 10^{15}\phi_{-1}^{1/2}\delta_{10}B_4^{*1/2}n^{*1/2}_{\rm t,15}f_{\rm v,-8}^{1/2}R_{14}^{-1}f_{\rm B}^{1/2}\quad {\rm Hz}. \quad (13)$$

Near the base of the jet, however, the putative dense clouds are possibly diamagnetic, confined by the magnetic field rather than penetrated by it, and also their covering factor may be small. Thus, we do not expect to observe Faraday rotation at optical wavelengths, unless the clouds are disrupted and fill the jet very quickly. On the other hand, at centimeter radio wavelengths (whose emission region is at $R\gtrsim 10^{19}$ cm), such clouds would almost certainly fill the jet, i.e. $f_{\rm v}\sim 1$. Then at $R=10^{19}$ cm and $\nu=5$ GHz, $\chi=(9\times 10^{-7})n_{\rm t}^*B_4^*f_{\rm B}\phi_{-1}\delta_{10}^2$ rad.

VLBI observations at 5 GHz have established that in most BL Lac objects the magnetic field in the radio jet is aligned transverse to the local jet direction (Cawthorne et al. 1991; Gabuzda et al. 1994). Hence we can set $\chi\lesssim 1$ rad, leading to an upper limit on the average density of thermal material at the base of the jet,

$$n_{\rm t}^*f_{\rm v}\lesssim 10^6B_4^{*,-1}f_{\rm B}^{-1}\phi_{-1}^{-1}\delta_{10}^{-2}\quad {\rm cm}^{-3}. \quad (14)$$

The kinetic power corresponding to the above average density is $L_{\rm kin,t}\lesssim (2\times 10^{42})(B_4^*f_B\phi_{-1})^{-1}$ erg s^{-1}. Hence, if $B_4^*f_{\rm B}\phi_{-1}L_{\rm jet,46}\gtrsim 2\times 10^{-4}$, then $L_{\rm kin,t}<L_{\rm jet}$. This means that most of the energy in the jet is carried by the relativistic particles and magnetic field, and that the bulk kinetic energy of the thermal matter (and low energy relativistic electrons) is insufficient to form a significant energy reservoir to compensate for radiative and expansion losses. A conservative estimate of the dissipation in form of observed radiation in BL Lacs would in fact lead to comoving luminosities $L_{\rm rad,Comp}\sim (8\times 10^{42})L_{\rm rad,45}\delta_5^{-3}$ erg s^{-1} (where a typical observed luminosity $L_{\rm rad,45}$ has been assumed) while the luminosity carried by the relativistic emitting component and magnetic field at pc scales imply $L_{\rm B}+L_{\rm kin,nt}\gtrsim 10^{44}$ erg

s^{-1} (e.g. Celotti & Fabian 1993). We note that these latter estimates strictly refer to the case of BL Lac objects, i.e. low power and weak–lined sources.

At face value eq. (14) gives a powerful constraint on the presence of thermal material in radio emitting jets, but it depends strongly on the factor $f_{\rm B}$, which describes the reduction in Faraday rotation due to reversals in field direction. In the bright VLBI knots, the field has a large-scale ordering imposed by shocks (Aller et al. 1985; Wardle et al. 1994) and there is no information about the fine grained structure. In the inter-knot regions, it is plausible to describe the field structure as nearly randomly oriented cells of uniform magnetic field. Then $f_{\rm B} \sim N^{-\frac{1}{2}} \sim p/0.7$ where N is the number of cells in a resolution element and p is the observed fractional polarization. In cases where the inter–knot polarization has been measured, p is typically a few per cent implying $f_{\rm B} \sim$ a few $\times 10^{-2}$.

This value is probably appropriate for BL Lac objects where both the predominantly transverse magnetic field and the magnetic field strength inferred for the radio emitting region are consistent with conservation of flux ($B \propto 1/R$) and a field of $\sim 10^4$ G at the base of the jet (at $\sim 10^{14}$ cm). However, it may be seriously overestimated for quasars, where the magnetic field is often longitudinal and may be dominated by sheared loops field ($f_{\rm B} \simeq 0$), as described by Begelman, Blandford & Rees (1984). Indeed it is possible that the observed differences in the VLBI polarization properties of quasars and BL Lac objects (e.g. Roberts & Wardle 1990; Gabuzda et al. 1992) is associated with the presence or absence of significant quantities of thermal material in/around the jets.

Finally, it is interesting to note that the estimates of the relativistic particle density on these observational scales give $n_{\rm nt} \sim 10^3 \gamma_{\rm e,min}^{-1}$ cm^{-3}, which is consistent with the maximum density derived from the total power constraints for $\gamma_{\rm e,min} \gtrsim 100$ (e.g. Celotti & Fabian 1993).

5.5 Emission

Any absorbed radiation would be reprocessed by the thermal gas. It would then be typically re-emitted, as continuum, lines and edges, at an energy δkT, with an intensity amplified by relativistic beaming. We refer to Kuncic et al. (1997) for a detailed study of the radiative properties and spectra emitted by clouds embedded in a non–thermal radiation field. Most of the radiation is expected to be optically thin continuum and lines plus edges concentrated in the EUV band and highly broadened by the bulk motion of the emitting gas.

Here, for simplicity, we estimate the emission by a thermal plasma at a temperature $\sim 10^5 T_5$, in the case of optically thin emission. This would be observed as (beamed) radiation up to a cut–off frequency $\nu_{\rm cut} \simeq (2 \times 10^{16}) T_5 \delta_{10}$ Hz. This luminosity can become energetically significant and potentially observable if $\nu_{\rm cut} L_{\nu,\rm brem}$ (erg s^{-1}) is comparable with the observed spectral power, say $\simeq 10^{46} L_{\rm rad,46}$. The corresponding density of thermal gas that is required to produce $L_{\rm rad,46}$ is then

$$n_{\rm t} \gtrsim (4 \times 10^{17}) L_{\rm rad,46}^{1/2} \delta_{10}^{-3/2} T_5^{1/4} \phi_{-1}^{-1} f_{\rm v,-8}^{-1/2} R_{14}^{-3/2} \exp(0.48 \nu_{16}/\delta_{10} T_5)^{1/2} \quad {\rm cm}^{-3}, \quad (15)$$

where the exponential term is of the order of unity.

A further constraint on the amount of thermal material in relativistic jets can be derived from the absence of any observed Compton scattered component in the soft X–ray band of radio–loud sources. In fact, Sikora et al. (1996a) pointed out that the presence of cold electrons in the jet could be detected through the effect of Comptonization of any external radiation field. In the case of optical/UV blue bump photons, this scattered component would contribute to the soft X–ray emission. On the other hand, the lack of any spectral signature in this band imposes a limit on the amount of cold material comoving with the jet, which can be translated into $n_{\rm t} \lesssim (2 \times 10^{17}) \phi_{-1}^{-2} L_{\rm softX,46} L_{\rm UV,45}^{-1} \Gamma_{10}^{-2} f_{\rm v,-8}^{-1} R_{14}^{-1}$ cm^{-3}. This limit again implies a minimum level of 'clumpiness', with values of $f_{\rm v}$ similar to those already derived, at least for distances R where an intense external radiation field is likely to be present (typically out to $R \lesssim 0.1$ pc).

6 SUMMARY AND RESULTS

In this Section, the limits derived so far are considered globally. In particular, we compare the relative importance of emission, absorption and Faraday rotation due to thermal material at different frequencies and distances along a relativistic jet.

The constraints on cool clouds of thermal material immersed in an AGN jet are plotted in Fig. 1 in a density versus size ($n_{\rm t}$ vs. r) parameter space diagram. The limits are estimated in the inner jet, at a distance $R = 10^{14} R_{14}$ cm. In Fig. 2 only the tightest physical constraints are reported at different distances along the jet, namely $R = 10^{14} R_{14}$, $10^{16} R_{16}$, $10^{18} R_{18}$ cm, where jets become spatially resolved by VLBI (from the top to the bottom panel, respectively). A filling factor of $f_{\rm v} = 10^{-8}$ has been adopted at all R. Each line is labelled as explained in the figure caption of Fig. 1 and throughout the previous sections. For comparison, one can locate in the same plane the physical properties inferred for broad–line clouds, i.e. $n \sim 10^{8-11}$ cm^{-3}, $r \sim 10^{12}$ cm at $R \sim 0.1$ pc, for filling factors ~ 10 times higher (e.g. Netzer 1990).

6.1 Theoretical limits

The gravitational scaleheight is the strongest upper limit on the cloud size for $R \lesssim 10^{16}$ cm, with $h_{\rm grav} \sim 10^7$ cm (at $R = 10^{14}$ cm) and $\sim 10^{11}$ cm (at $R = 10^{16}$ cm). As already discussed, however, the typical scaleheight is likely to be affected by much stronger radiative, dynamical and magnetic forces acting on the clouds. For effective accelerations of the order of $a \gtrsim 10^{6-8} g$, the existence of any clumped thermalized structure at these distances is precluded. At $R > 10^{16}$ cm, however, the requirement that the gas responds to any perturbation on timescales smaller than $t_{\rm dyn}$ places a more stringent limit on r than does $h_{\rm grav}$, giving $r \lesssim 10^{13}$ cm.

The lowest limits on r are set by the magnetic field diffusion scales to dimensions of the order of 10 to 10^3 cm. For low densities, the cloud size starts to be comparable with the collisional mean free path and any low frequency absorption is likely to be dominated by induced Compton scattering rather than bremsstrahlung absorption. While thermal diffusion from the relativistic phase can also act on such spatial

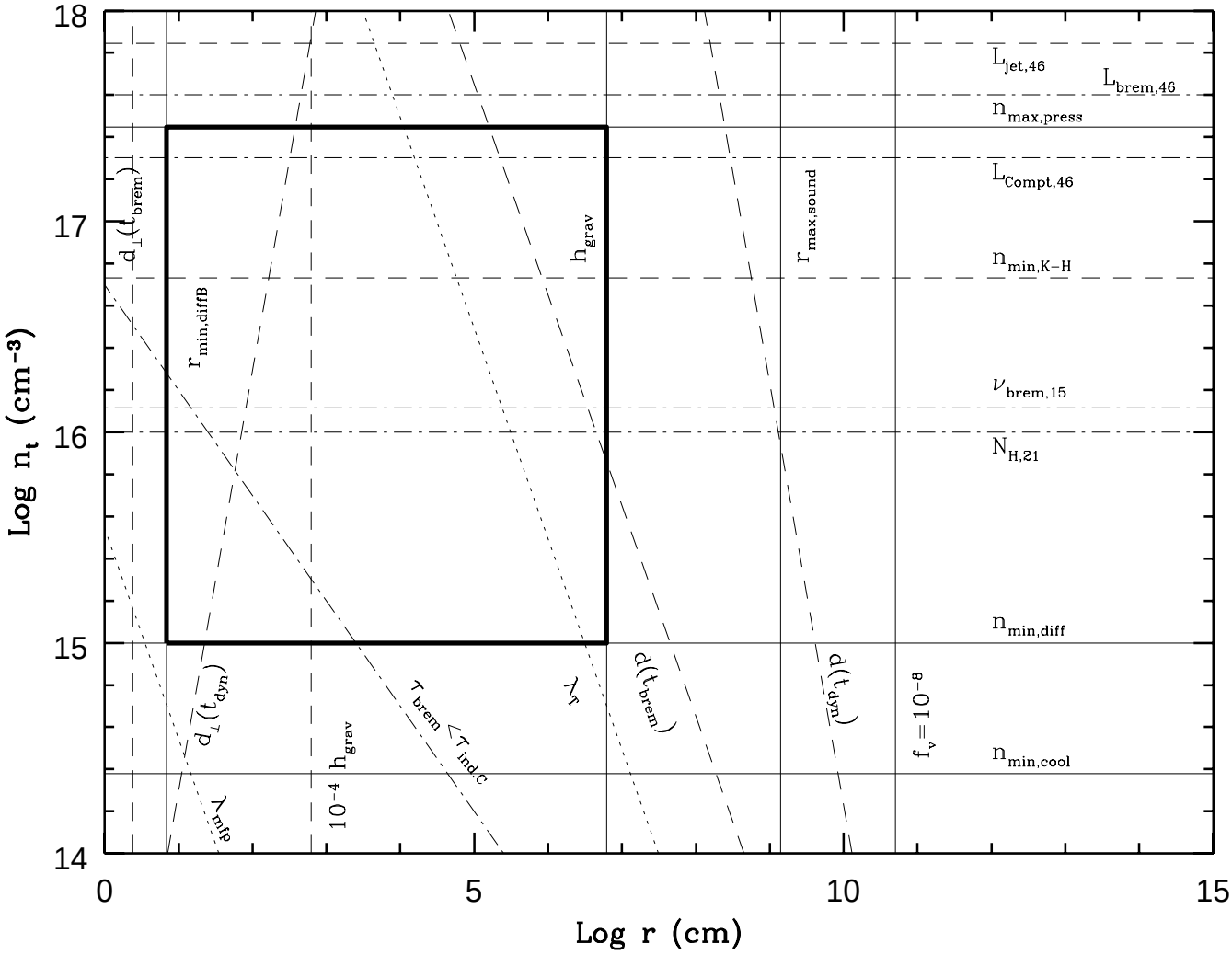

Figure 1. Parameter space diagram (density, $n_{\rm t}$, versus thickness, r) for thermal material in relativistic AGN jets at distance $R = 10^{14} R_{14}$ cm, with a temperature 10^5 K and a volume filling factor 10^{-8}. The various constraints discussed at length in the text are plotted here and identified by the following labels:
$n_{\rm max,press}$ — density at which thermal pressure balances confining magnetic pressure;
$n_{\rm min,diff}$ — minimum density for gas to remain cool in the presence of non–thermal diffusion;
$r_{\rm min,diffB}$ — minimum scalesize of structure unaffected by magnetic diffusion;
$h_{\rm grav}$ — gravitational pressure scaleheight;
$r_{\rm max,sound}$ — maximum sound–crossing scalesize for pressure equilibrium on a dynamical timescale;
$L_{\rm jet,46}$ — total jet power implies an upper limit on particle kinetic energy density;
$L_{\rm brem,46}$ — density responsible for bremsstrahlung emission comparable to observed spectral luminosity;
$L_{\rm Comp,46}$ — density producing a Comptonization luminosity comparable to observed spectral power;
$n_{\rm min,cool}$ — minimum density for 2–body processes to cool gas more efficiently than particle–photon processes;
$n_{\rm min,K-H}$ — minimum density at which Kevin–Helmholtz instability is suppressed;
$N_{\rm H,21}$ — neutral hydrogen column density limit;
$\nu_{\rm brem,15}$ — density corresponding to a spectral turnover at optical frequencies due to bremsstrahlung absorption;
$d(t)$ — non–thermal diffusion depth during a timescale t ($t_{\rm dyn}$ and $t_{\rm brem}$ are the dynamical and cooling timescales);
$d_\perp(t)$ — same as $d(t)$, but for non–thermal diffusion transverse to the magnetic field lines;
$\lambda_{\rm T}$ — effective mean–free–path for collisions between non–thermal and thermal particles;
$\lambda_{\rm mfp}$ — mean–free–path for collisions between thermal particles only;
$\tau_{\rm brem} < \tau_{\rm indC}$ — relative optical depths due to bremsstrahlung absorption and induced Compton scattering;
$f_{\rm v}$ — (spherical) cloud dimension corresponding to a filling factor $f_{\rm v}$. Continuous lines indicate the strongest limits; dashed lines correspond to constraints which can be overcome by different assumptions or cannot be determined with precision; dash–dot lines show observational limits; and dotted lines refer to physical quantities. The area enclosed by the heavy set lines defines the resultant parameter subspace allowed by the relevant constraints.

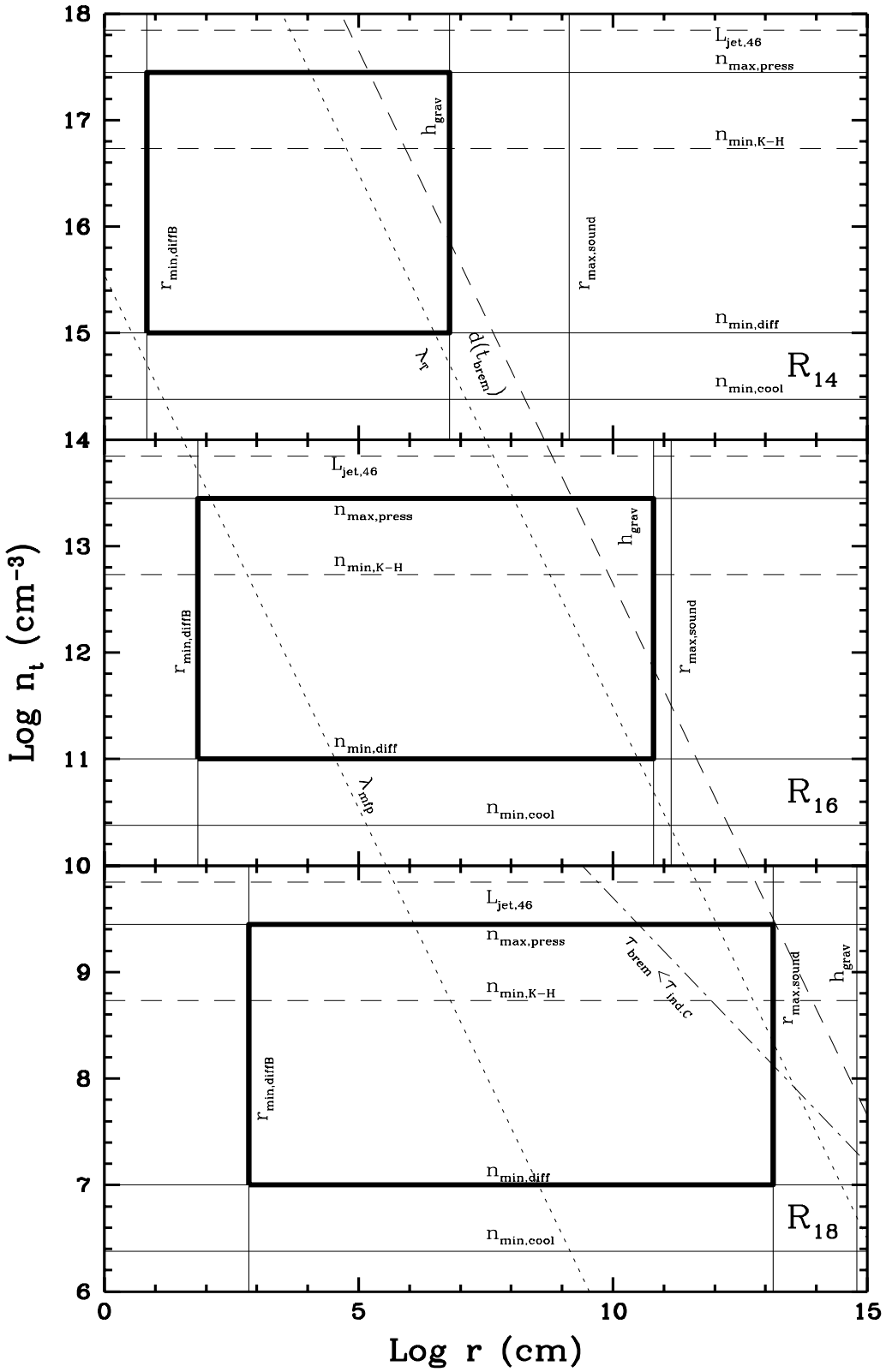

Figure 2. Parameter space diagram (density, $n_{\rm t}$, versus thickness, r) for thermal material in relativistic AGN jets at distances $R = 10^{14}R_{14}$ cm (top panel), $10^{16}R_{16}$ cm (middle panel) and $10^{18}R_{18}$ cm (bottom panel) and with a constant temperature 10^5 K and constant volume filling factor 10^{-8}. Only the tighter physical constraints are reported here. A complete summary of the limits, including the observational ones, is included in Fig. 1, with the same labels and type of lines. The area enclosed by the heavy set lines defines the resultant parameter subspaces allowed by the relevant constraints.

scales, this effect does not pose a serious threat to the survival of cool clouds provided their density exceeds $n_{\rm min,diff}$ (which is estimated here for a maximum density of the relativistic external plasma, $n_{\rm nt} \sim 10^9$ cm^{-3}). Furthermore another constraint on the minimum density of thermal material is given by $n_{\rm min,cool}$, which is set by the requirement that the gas can cool in the intense radiation field that is expected to prevail within 10^{16-17} cm.

Finally, cloud pressures cannot exceed the confining magnetic one and this constrains the thermal material to $n_{\rm t} \lesssim n_{\rm max,press}$. Note however that this has been calculated for diamagnetic clouds and neglecting any internal radiation pressure. It is also relevant to stress here that both the pressure and the total jet power limits are linearly dependent on the assumed jet power.

The allowed parameter space is confined within the thick box in each panel of Figs. 1 and 2. The limits imply that the typical densities at which cold clumped matter can exist in the jet environment scale with distance as $\sim R^{-2}$ and span about two–three orders of magnitude (at each distance).

The other constraints discussed in the paper and reported in Figs. 1, 2 depend on the volume filling factor as well as the dynamics of the clouds (e.g. the Kelvin–Helmholtz stability limit). In general they indicate that filling factors of the order of 10^{-8} are necessary for cold material to have the range of densities required to survive in the jet environment.

To summarize our findings, relatively cold, thermal material with small volume filling factors can exist in the relativistic environment of an AGN jet under the considered conditions at all scales $R \lesssim 1$ pc, when confined and insulated by a strong magnetic field. Dynamically, these structures can become unstable if they are subjected to an acceleration phase on dynamical timescales.

6.2 Observational predictions

Thermal material with the properties inferred above should produce reprocessing signatures in the observed spectra. In the inner jet, cool material could absorb the locally produced radiation field up to optical frequencies and re-emit this energy as quasi–thermal UV radiation at levels comparable to the observed flux, for $f_{\rm v} \gtrsim 10^{-8}$. This radiation would probably contribute and possibly exceed any component from the optical to the EUV–soft X–ray spectral band in radio–loud sources.

At higher energies, thermal gas can manifest itself through photoelectric absorption in the soft X–ray band. The observational limits on the column density in neutral hydrogen are quite tight, typically $N_{\rm H} \lesssim 10^{21}$ cm^{-2}, and are compatible with the range of gas parameters found only if either a significant fraction of the cold material is ionized or the covering factor is much lower than 1 or the soft X–ray emitting region is not located in the inner part of the jet. Furthermore, a Comptonized component is expected to be observable in the soft X–ray band, from material with $f_{\rm v} \gtrsim 10^{-8}$. For $R \gtrsim 10^{16}$ cm, however, these radiative features are not observable unless $f_{\rm v} \gg 10^{-8}$.

Finally, we note that the observational constraints on Faraday rotation, which are particularly relevant to BL Lac objects, correspond to the lower end of the density range in each panel in Fig. 2, assuming that a filling factor $f_{\rm v} \sim 10^{-8}$ and $f_{\rm B} \sim 1$ remain constant at all R. Values of $f_{\rm v}$ which are $\lesssim 10^{-9}$ or smaller values of $f_{\rm B}$ would therefore be incompatible at all R with the observational results derived on scales $\sim 10^{19}$ cm (see however the discussion in Section 5.4). We note that even if cooled electrons are not confined and fill the jet, Faraday rotation measures could detect their presence.

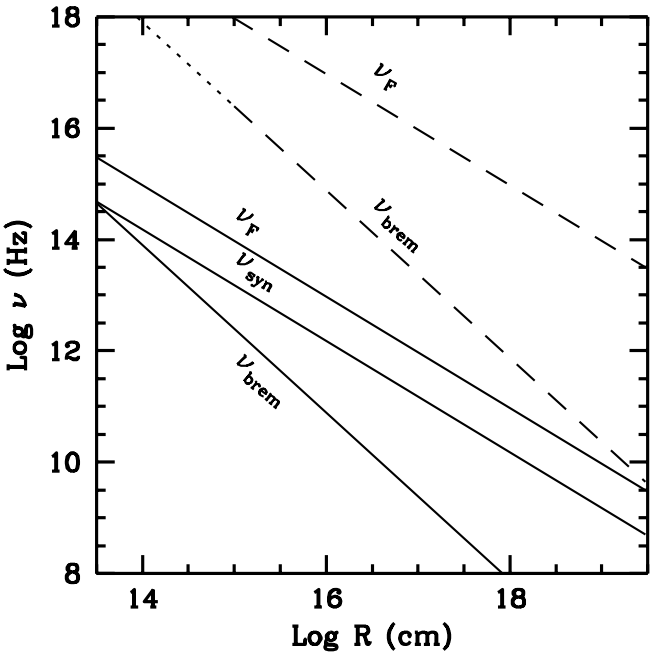

Figure 3. The dependence of the (observed) synchrotron ($\nu_{\rm syn}$) and bremsstrahlung ($\nu_{\rm brem}$) absorption frequencies and the typical frequency at which Faraday rotation is measurable ($\nu_{\rm F}$) on the distance R along the jet. Volume filling factors $f_{\rm v}$, possibly ranging from small values in the inner part of the jet ($\sim 10^{-8}$) to even ~ 1 at the observed scales, have been considered and represented by continuous and dashed lines respectively. A Doppler factor δ_{10} has been adopted. The dotted line section indicates the bremsstrahlung absorption frequency computed in the Rayleigh–Jeans limit (which overestimates $\nu_{\rm brem}$ at most by a factor ~ 4 at R_{14})

Fig. 3 shows the relative importance of radiative absorption processes and Faraday rotation at different frequencies and distances along the jet, showing which radiative signature is most likely to be observable in different spectral bands and at different resolution.

For densities of thermal material in the allowed parameters space of Fig. 2, synchrotron self–absorption by the non–thermal relativistic plasma is the most effective absorption process, for filling factors of the thermal gas $f_{\rm v} \lesssim 10^{-8}$ (and the minimum thermal gas density allowed by the limits reported in Fig. 2). Faraday rotation can possibly affect radiation at frequencies a factor ~ 4 above the synchrotron self–absorption ones. For higher values of $f_{\rm v}$, as might be in the more external jet regions, Faraday rotation can be the strongest observational signature of the presence of thermal gas (note however that the estimate of this effect is based on an assumed $f_{\rm B} \sim 1$). Absorption by bremsstrahlung would be more effective in depleting photons in the IR to UV bands up to a distance which depends on $f_{\rm v}$.

As already discussed, any radiative signature (and in particular any absorption feature) critically depends on the relative location of the region mostly emitting at each frequency. In fact if the jet structure is inhomogeneous, the observed spectra could be the superposition of the emission from different regions of the jet, which contribute differently at each frequency. As an example, in the parametric model developed by Ghisellini & Maraschi (1989) the region typically dominating the emission in the near IR–optical–UV bands is located at about $R \sim 10^{16-17}$ cm, as suggested by simple variability timescale arguments (which in fact sets upper limits on the size of the emitting region but not on its location along the collimated jet). In this case then clouds would need to have rather high covering and filling factors to produce detectable signatures.

6.3 Energetic implications

At all distances, the theoretical limits on the density of thermal material are consistent with its kinetic power not exceeding the total jet power, and imply that the gas cannot fill the jet for more than $\sim 10^{-5}$ of its volume. For the adopted value of filling factor, its contribution can be up to 25 per cent of the total power carried by the jet.

From an observational point of view, however, the lack of thermal signatures (in absorption or emission) from radio to soft X–ray energies in radio–loud AGN, suggests that any thermal material is confined in an even smaller volume. Therefore the reservoir of energy which can be carried as kinetic power of cold thermal gas is unlikely to be energetically important, unless either $\Gamma \ll 10$ (which would make AGN jets more closely resemble those of young stars or compact objects) or some caveats about the lack of observed features are invoked.

7 CONCLUSIONS

There is strong evidence for the presence of at least 10–100 $M_\odot$ of thermal gas in the central regions of radio–loud AGN. This non–relativistic material may be closely associated with relativistic jets either externally, as is probably the case with narrow line emitting gas, or possibly internally, as is the case with jets on stellar scales (e.g. SS 433).

Thermal material trapped in the central environs of AGN is likely to be magnetically confined, as suggested by Rees (1987) and Emmering et al. (1992) (see also the models by Ghisellini & Madau 1996 for the γ–ray emission and de Kool & Begelman 1995 for broad absorption line gas in quasars). A strong magnetic field permits the presence of gas that is multiphase in nature, with 'cold' gas confined and thermally insulated from non–thermal emitting plasma. The spatial distribution of the cold component is determined by the configuration of the field, so that filamentary structures would probably prevail. Moreover, the boundary of any material confined in such a way could be a preferential location for acceleration of particles to relativistic energies, through e.g. magnetic reconnection.

In this paper, we have examined the physical conditions in the environment of relativistic AGN jets containing both non–thermal and thermal matter and we have found that the 'cold' component could conceivably be present at all distances throughout the jets, from the innermost regions out to parsec scales, over several orders of magnitude in density and dimension. The strongest constraints on the physical properties of such cold gas are imposed by non–thermal diffusion effects associated with Coulomb collisions with fast particles, the requirement of pressure equilibrium with the ambient magnetic field, the gravitational pressure scaleheight and, on the smallest scales, magnetic diffusion effects. Unfortunately, the lack (so far) of radiative spectral signatures, such as emission and absorption features as well as Faraday rotation measures, in the observed non–thermal spectra limits the filling factor of thermal gas to such small values that it cannot constitute an important component in the overall energy budget of jets in radio–loud AGN. We hope that future broadband, spectroscopic and polarimetric observations of blazars will either further constrain the above result or possibly reveal the predicted thermal reprocessing features.

We note that while in our analysis we have adopted a reference jet power of 10^{46} erg s^{-1}, the constraints would be even stronger if higher luminosities (as estimated in some powerful jets) were considered. It is also important to point out that our findings are especially relevant for thermal material in the jet of weak–lined sources as BL Lacs. In fact, both their estimated total power is lower and observational constraints (in terms of Faraday limits and optical/UV thermal emission) are certainly tighter. This seems to support the view that indeed the environment of weak blazars lacks significant amounts of thermal material.

The absence of an energetically significant cold thermal component is an important constraint on jet models, somehow in agreement with several other suggestions of the deficiency of low energy particles. All these indications point to a highly efficient (re–)acceleration mechanism operating in the jet, either in form of e.g. reconnection, shocks or heating by radiative absorption, which would have to maintain the bulk of particles at least at mildly relativistic energies.

ACKNOWLEDGMENTS

We acknowledge Gary Ferland for the use of his code CLOUDY. For financial support, thanks are due to the Italian MURST (AC), the Australian DIST (ZK), the Royal Society (MJR). JFCW acknowledges the John Simon Guggenheim Memorial Foundation for a Fellowship.

REFERENCES

Aller H.D., Aller M.F., Hughes P.A., 1985, ApJ, 298, 296
Begelman M.C., Blandford R.D., Rees M.J., 1984, Rev. Mod. Phys., 56, 255
Biretta J.A., Sparks W.B., Macchetto F., Capetti A., 1995, BAAS, 187, 5016
Blandford R.D., 1993, in Burgarella D., Livio M., O'Dea C.P., eds, Astrophysical Jets. Cambridge Univ. Press, Cambridge, p. 15
Blandford R.D., Königl A., 1979, ApJ, 232, 34
Blandford R.D., Levinson A., 1995, ApJ, 441, 79
Blandford R.D., Rees M.J., 1978, in Wolfe A.M., ed, Proc.

Pittsburgh Conf. on BL Lac Objects. Univ. of Pittsburgh Press, Pittsburgh, p. 328
Bregman J.N., 1990, A&AR, 2, 125
Canizares C.R., Kruper J., 1984, ApJ, 278, L99
Capetti A., Axon D.J., Macchetto F., Sparks W.B., Boksenberg A., 1996, ApJ, 469, 554
Cappi M., Matsuoka M., Comastri A., Brinkmann W., Elvis M. Palumbo G.G.C., Vignali C., 1997, ApJ, in press
Cawthorne T.V., Wardle J.F.C., Roberts D.H., Gabuzda D.C., 1993, ApJ, 416, 519
Celotti A., Fabian A.C., 1993, MNRAS, 264, 228
Celotti A., Fabian A.C., Rees M.J., 1992, MNRAS, 255, 419
de Kool M., Begelman M.C., 1995, ApJ, 455, 448
de Kool M., Begelman M.C., Sikora M., 1989, ApJ, 337, 66
Eilek J.A., Caroff L.J., 1979, ApJ, 233, 463
Elvis M., Fiore F., Wilkes B.J., McDowell J.C., Bechtold J., 1994, ApJ, 425, 103
Elvis M., Mathur S., Wilkes B.J., Fiore F., Giommi P., Padovani P., 1997, in Proc. of IAU Coll. 159, Emission Lines in Active Galaxies: New Methods and Techniques, in press
Emmering R.T., Blandford R.D., Shlosman I., 1992, ApJ, 385, 460
Gabuzda D.C., Cawthorne T.V., Roberts D.H., Wardle J.F.C., 1992, ApJ, 338, 40
Gabuzda D.C., Mullan C.M., Cawthorne T.V., Wardle J.F.C., Roberts D.H., 1994, ApJ, 435, 140
Ghisellini G., Madau P., 1996, MNRAS, 280, 67
Ghisellini G., Maraschi L., 1989, ApJ, 340, 181
Ghisellini G., Guilbert P.W., Svensson R., 1988, ApJ, 334, L5
Ghisellini G., Bodo G., Trussoni E., Rees M.J., 1990, ApJ, 362, L1
Grandi P., et al., 1997, A&A, submitted
Königl A., 1989, in Maraschi L., Maccacaro T., Ulrich M.–H., eds, BL Lac Objects. Springer–Verlag, p. 321
Königl A., Kartje J.F., Kahn S.M., Chorng–Yuan Hwang, 1995, ApJ, 446, 598
Krolik J.H., Kallman T.R., Fabian A.C., Rees M.J., 1985, ApJ, 295, 104
Kuncic Z., Blackman E., Rees M.J., 1996, MNRAS, 283, 1322
Kuncic Z., Celotti A., Rees M.J., 1997, MNRAS, 284, 717
Madejski G.M., Mushotzky R.F., Weaver K.A., Arnaud K.A., Urry C.M., 1991, ApJ, 370, 198
Mathews W.G., Ferland G.J., 1987, ApJ, 323, 456
Mirabel I.F., Rodriguez L.F., 1996, in Tsinganos K.C., ed, Solar and Astrophysical Magnetohydrodynamical Flows. Kluwer Academic Publisher, The Netherlands, p. 683
Nesci R., Massaro E., 1996, IAU Circ. 6457
Netzer H., 1990, in Courvoisier T.J.-L., Mayor M., eds, Active Galactic Nuclei, 20^{th} SAAS–FEE Course. Springer–Verlag.
Phinney E.S., 1987, in Zensus J.A., Pearson T.J., eds, Superluminal Radio Sources. Cambridge Univ. Press, Cambridge, p. 301
Rawlings S.G., Saunders R.D.E., 1991, Nat, 349, 138
Rees M.J., 1987, MNRAS, 228, 47p
Roberts D.H., Wardle J.F.C., 1990, in Zensus J.A., Pearson T.J., eds, Superluminal Radio Sources. Cambridge Univ. Press, Cambridge, p. 193
Robinson A., Corbett E., 1996, IAU Circ. 6463
Sikora M., Begelman M.C., Rees M.J., 1994, ApJ, 421, 153
Sikora M., Madejski G., Moderski R., Poutanen J., 1996a, ApJ, submitted
Sikora M., Sol H., Begelman M.C., Madejski G.M., 1996b, MNRAS, 280, 781
Stickel M., Fried J.W., Kühr H., 1993, A&AS, 98, 393
Vermeulen R.C., 1993, in Burgarella D., Livio M., O'Dea C.P., eds, Astrophysical Jets. Cambridge Univ. Press, Cambridge, p. 241
Vermeulen R.C., Ogle P.M., Tran H.D., Browne I.W.A., Cohen M.H., Readhead A.C.S., Taylor G.B., 1995, ApJ, 452, L5
Walker R.C., Romney J.D., Benson J.M., 1994, ApJ, 430, L45
Wardle J.F.C., Cawthorne T.V., Roberts D.H., Brown L.F., 1994, ApJ, 437, 122
Whittle M., Saslaw W.C., 1986, ApJ, 310, 104
Wills B.J., 1996, in Kundt W., ed, Jets from Stars and Galactic Nuclei. Springer–Verlag, Heidelberg
Wilson A., 1993, in Burgarella D., Livio M., O'Dea C.P., eds, Astrophysical Jets. Cambridge Univ. Press, Cambridge, p. 121